

ANGLED BURIED CONTACTS: A FRONT CONTACTING SCHEME FOR HIGH EFFICIENCY CELLS WITH LOW SHADING LOSSES

Michelle McCann, Claudia Strümpel, Holger Knauss, Thomas Pernau*, Engelbert Lemp and Peter Fath
University of Konstanz, Faculty of Physics, 78457 Konstanz, Germany, email:Michelle.McCann@uni-konstanz.de
*Now at centrotherm Photovoltaics, Johannes-Schmid-Str. 3, 89143, Blaubeuren, Germany.

ABSTRACT: In this paper, we present the Angled Buried Contact (ABC) cell design. The design is for an easily realised front metallisation scheme that results in negligible shading. The ABC cell process does not require any additional processing steps compared to a standard buried contact process, rather the process is slightly simplified. The process is equally suited to multi- and mono-crystalline silicon. In this paper we present process developments and some initial cell measurements. We have demonstrated a proof of the new concept and, compared to buried contact reference cells, the ABC cells resulted in a maximum increase in J_{sc} of 0.7mA/cm^2 .

Keywords: Angled, Buried Contacts, Shading

1 INTRODUCTION AND BACKGROUND

The conventional buried contact solar cell process is a high efficiency process that was first introduced by Wenham and Green in the 1980s [1]. Buried contact cells on single crystalline silicon are produced commercially by BP Solar at facilities in Tres Cantos, Spain, where over 80MW_p have been produced since 1992 [2]. At the University of Konstanz, excellent cell results have been realised on large area multi-crystalline silicon wafers, including a cell with an efficiency of 17.6% [3] and an average (of 111 cells over a full brick) of 16.2% [4]. The major advantages of buried contact cells over screen printed cells include a selective emitter structure and reduced shading losses. Shading losses for screen printed cells are typically in the range 7-8%, for buried contact cells this is reduced to approximately 4%. A buried contact cell is shown schematically in Figure 1. A typical groove is approximately $20\mu\text{m}$ wide and $40\mu\text{m}$ deep [5, 6].

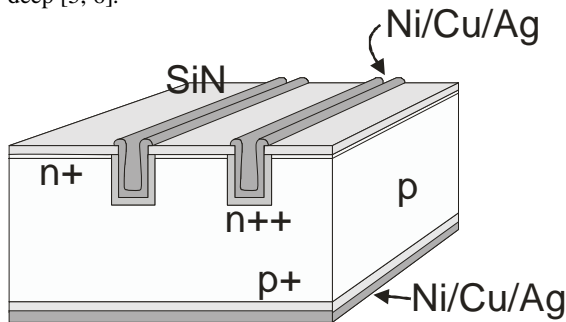


Figure 1: Schematic of a buried contact solar cell. The front metal contacts are buried and the front surface has a selective emitter structure with a light diffusion (n^+) on the front surface and a heavy diffusion (n^{++}) in the grooves. Front and rear metal contacts are formed by electroless plating of Ni, Cu and Ag.

Despite the reduced shading losses in the buried contact cell, there is still room for improvement. For example, if the front surface shading of the 17.6% cell mentioned above was reduced from 4% to 0%, simple calculations show that an increase in J_{sc} of 1.5mA/cm^2 (to 37.4mA/cm^2) could be expected. This is equivalent to an absolute efficiency improvement of 0.8%.

This potential improvement in efficiency was motivation for the design of the angled buried contact

(ABC) cell, which forms the basis of this work. The ABC cell has two main advantages. Firstly, it allows negligible shading losses but maintains front side metallisation and secondly, it is very similar to a conventional buried contact cell, which simplifies the realisation. The key to the ABC concept is angled grooves in combination with a directionally deposited silicon nitride. The silicon nitride acts as a mask for the heavy diffusion and ensures that only the undersides of the grooves will be metallised by the electroless plating. The metal contacts are hidden inside the angled grooves, as depicted in Figure 2.

In some respects, the ABC design is a variation of the “off-axis” concept proposed by Wenham and Green in 1991 [7]. The processing of off-axis cells is, however, significantly more complicated and requires non-standard wafers.

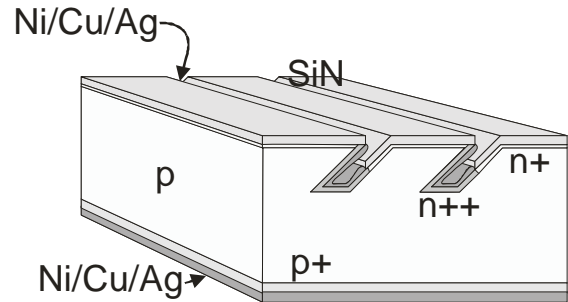


Figure 2: Design of the angled buried contact (ABC) solar cell. Like a conventional buried contact cell, the ABC cell has a selective emitter structure with a light diffusion (n^+) on the front surface and a heavy diffusion (n^{++}) in the grooves. In contrast to the conventional buried contact design, the front surface grooves are angled into the wafer, resulting in negligible reflection losses.

2 CELL PROCESS

In the following, we outline one possibility for producing ABC cells. The process is based on an adaptation of the hybrid screen print / buried contact process, which was developed at the University of Konstanz for multi-crystalline silicon [5]. Groove formation is the first step. The grooves are angled into the wafer and the final silicon-metal contact area will depend on both the angle and the depth of the groove.

The next steps are a light phosphorous diffusion and deposition of a PECVD SiN_x layer. The nitride deposition is directional and only the upward-facing surfaces are coated, leaving the remainder of the inside of the groove uncoated. A heavy phosphorous diffusion is then done, resulting in n^{++} regions in places not masked by the silicon nitride – i.e. in the hidden regions of the grooves. The remainder of the process is as for the standard hybrid screen print / buried contact process. A back surface field is formed by screen printing and firing an aluminium layer and metallisation in the front grooves and on the rear surface is by electroless nickel, copper and silver plating. The last step is edge isolation, which may be done using a laser or a dicing saw. The SiN_x acts as a mask during plating so that only the hidden regions of the groove are coated with metal. The process is compared to the hybrid screen print / buried contact process in Figure 3.

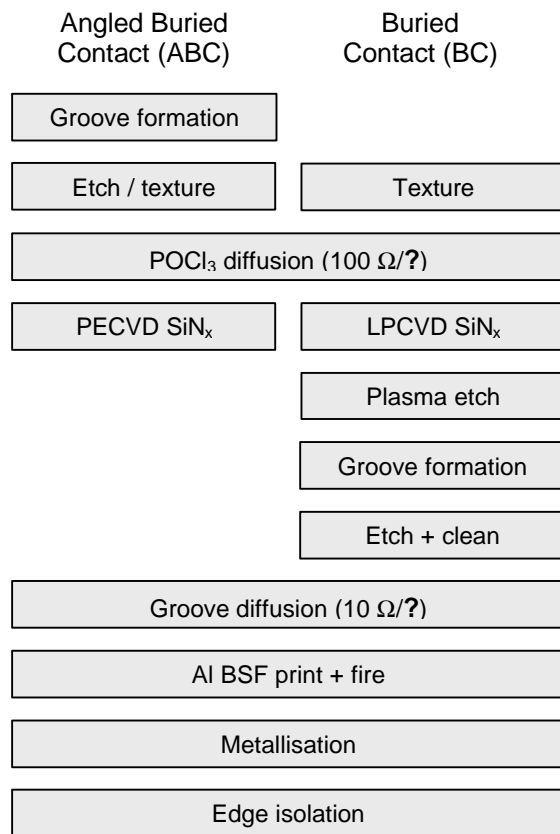


Figure 3: Comparison of the ABC cell process and the hybrid buried contact / screen print process. The ABC cell process has groove formation as the first step and uses PECVD instead of LPCVD SiN_x , and thereby avoids a cleaning step and the plasma etch, necessary to remove LPCVD SiN_x that has crept around the edge of the wafers and deposited on the front surface.

3 PROCESS DEVELOPMENT

Although the ABC cell process is similar to a conventional buried contact process, the inclusion of the angled grooves means that aspects of the process must be adjusted. Two of these aspects, groove formation and silicon nitride deposition are discussed below.

3.1 Groove Formation

The groove geometry is crucial for the ABC process. This is particularly the case during nitride deposition; when the wrong geometry may result in silicon nitride deposition in the hidden regions of the grooves, which will then be masked from the heavy phosphorous diffusion and later from metallisation. The groove geometry will also determine the mechanical stability of the overhanging edges and the contact and line resistance. Another aspect, which is discussed later in this paper, is internal reflection and absorption of long wavelength light from the metal-coated flank of the groove.

The first experimental work was done using a specially designed chuck on the dicing saw. Due to the layout of the dicing saw, we were limited to an angle of 30° and a 30µm thick blade. The first cuts were successful and we were able to achieve regularly spaced grooves of equal depth. Our first cell trials were done with relatively wide grooves (80µm) because we combined the damage etch after groove formation with a long saw damage removal etch. Separation of these two etches could result in much narrower grooves, which would also allow for more flexibility in the nitride deposition. The first cells also had relatively deep grooves (110-120µm). This is clearly unsuited to thinner wafers, for which the groove angle and finger spacing must be adjusted.

Figure 4 shows a scanning electron microscope image of a plated angled contact. The metal contact is on the hidden flank of the groove and covers approximately half of the base of the groove. The upward-facing region of the groove is free of metal, as expected. In this case over-plating at the top edge is evident. This is also the case for buried contact cells [6] and results in an increase in shading. With the angled buried contact design, it may be possible to adjust the nitride deposition conditions and / or the groove geometry so that there is some nitride deposition on the upper regions of this edge, which would eliminate this problem.

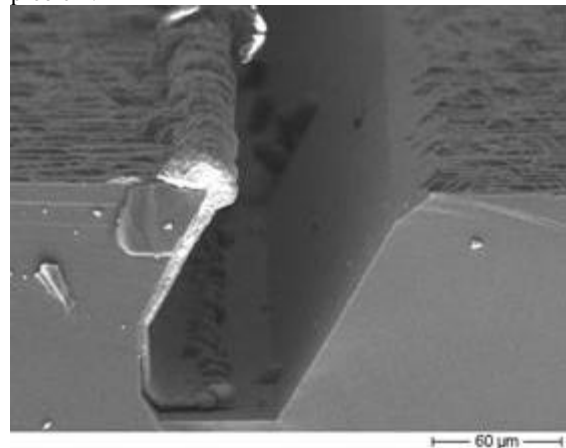


Figure 4: A multi-crystalline wafer with angled buried contact after electroless plating of Ni and Cu. Inside the groove the metal contact is only on the hidden flank, the up-ward facing regions of the groove are metal free, as expected. There is some over-plating evident. It may be possible to eliminate this by adapting the silicon nitride deposition conditions and / or the groove geometry.

3.2 Silicon Nitride Deposition

The PECVD silicon nitride must be adjusted for the ABC cell process. The nitride should be as directional as possible to ensure that the under-side of the grooves are eventually plated with metal. A higher directional component can be realised by reducing the deposition pressure. If the pressure is too low, however, we found that the nitride contained many pinholes. Pinholes are especially detrimental with the ABC concept because the cells are plated using electroless metallisation, which will also plate pinholes. We have done some first experiments to investigate the effect of the silicon nitride deposition pressure. Cells were made on untextured, Cz silicon with deposition pressures of 1.0, 1.3 and 1.7 torr. The results are shown in Table I. With the lowest deposition pressure J_{sc} was unacceptably low due to shading of the front surface from the many pinholes. The optimum deposition pressure appears to be in the region of 1.7 torr.

Deposition pressure (torr)	J_{sc} (mA/cm ²)	Pinhole density
1.0	5.3	High
1.3	34.9	Medium – low
1.7	35.3	Low

Table I: Results of the first optimisation of the silicon nitride deposition pressure. The J_{sc} values shown are for the best cell from each group. For the very low pressure deposition, the J_{sc} values are low due to excessive shading of the front surface from the many pinholes.

4 CELL RESULTS

We have produced cells on both Cz and mc silicon wafers using the process schematics shown in Figure 3. For the ABC cells, the finger grooves were angled at 30° to the wafer surface and were 70-80µm wide and 110-120µm deep. For first tests, the busbars were not angled into the wafer in order to simplify the IV measurements. The buried contact cells had narrower fingers; 40-50µm, but an equivalent depth; 100-110µm. The J_{sc} values are shown in Table I and Table II shows full IV results for the best cells made using silicon nitride deposition pressures of 1.3 and 1.7 torr. The cells were untextured and made on Cz silicon. As expected, compared to the buried contact reference cells, the ABC cells show an increased J_{sc} (0.4 and 0.7 mA/cm²). Surprisingly, the cells also had a reduced V_{oc} (8 and 11 mV) and fill factor (7 and 10 % absolute). The result is a reduced efficiency of the ABC cells in comparison to the buried contact reference cells.

Cell type	FF (%)	J_{sc} (mA/cm ²)	V_{oc} (mV)	η (%)
BC 1	77.9	34.2	607	16.2
ABC 1	70.9	34.9	599	14.8
Difference	-7.0	+0.7	-8	-1.4
BC 2	77.9	34.9	616	16.7
ABC 2	67.8	35.3	605	14.5
Difference	-10.0	+0.4	-11	-2.2

Table II: IV results for buried contact and angled buried contact cells. BC 1 and ABC 1 were made using a silicon nitride deposition pressure of 1.3 torr, BC 2 and ABC 2 with a deposition pressure of 1.7 torr.

The cells listed in Table II underwent a more detailed investigation. In the following, details of dark IV measurements, spectral response, reflectance, laser beam induced current (LBIC) and illuminated lock-in thermography (iLIT) measurements are discussed. Except where noted, the results shown are for ABC 2 and BC 2, the two cells made with a silicon nitride deposition pressure of 1.7 torr.

Dark measurements of the cells shown in Table II were made. The measurements did not fit well to the 2-diode model, which can be an indication for localised shunting [8]. Approximate fits to the 2-diode model indicated an increased R_{sh} for the ABC cells and an increased J_{02} . The increased R_{sh} may be due to localised breaking of the overhanging groove edge and shunting was further investigated with iLIT measurements (discussed in more detail below).

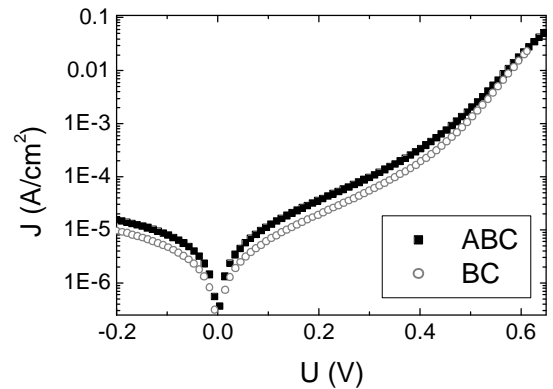


Figure 5: Dark IV curves for the angled buried contact (ABC) and buried contact (BC) cells. Approximate fits to these curves showed that the ABC cells have a higher shunt resistance and a higher J_{02} .

Figure 6 shows reflectance measurements and the IQE curves calculated from the reflectance and spectral response measurements. The ABC cell shows a reduced reflectance. This is an expected result, given that the metal fingers are largely hidden, and explains the increased J_{sc} . The total solar weighted reflectance of the ABC cell is 10.3%, a 2% absolute reduction compared to the buried contact cell. This is especially significant considering that the fingers on the ABC cell are almost twice the width of those on the buried contact cell.

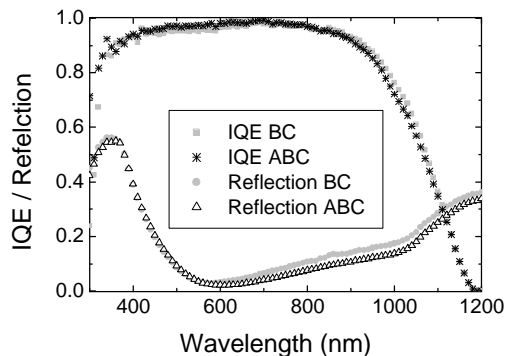


Figure 6: Reflection measurements and IQE curves. The ABC cell shows a reduced reflection (the solar weighted reflectance is reduced from 12.3 to 10.3%), which explains the increased J_{sc} values. The IQE curves are very similar.

The IQE curves for both cells are similar. The ABC cell shows a slightly better performance at shorter wavelengths and a slightly worse performance at longer wavelengths. Possible reasons for this are discussed below.

Illuminated, lock-in Thermography measurements [9,10] of both ABC cells listed in Table II were made. The results are shown in Figure 7 and indicate localised shunting, which is consistent with the dark IV measurements. The shunts were not visible under reverse bias, which implies that they are schottky shunts. It is possible that they formed as a result of localised breaking of the overhanging groove edge.

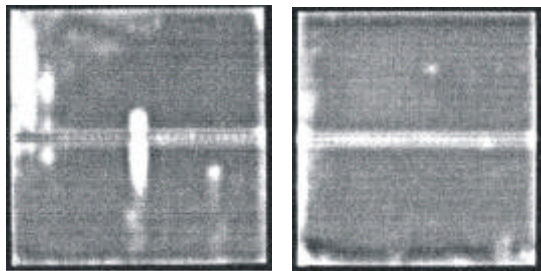


Figure 7: Thermography measurements of the two ABC cells listed in Table II. The white regions indicate warmer areas and therefore shunts. For both cells, localised shunts are evident.

Although the angled buried contacts have reduced shading losses compared to buried contacts, for long wavelength light, they have an increased effective width. This may actually result in increased losses for long wavelength light, for which the silicon-metal interface will not be transparent. In order to investigate this effect, high resolution LBIC mapping was done. Figure 8 shows a detail of (left) a buried contact groove and (right) an angled (up, in this picture) buried contact groove. The buried contact grooves are 40-50 μm wide and the angled buried contact grooves 70-80 μm wide.

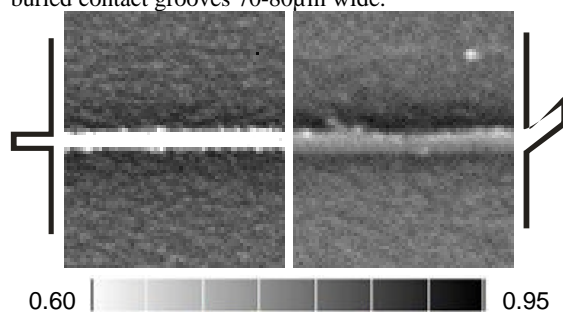


Figure 8: LBIC detail (made at a wavelength of 980nm) of a buried contact groove (left) and an angled buried contact groove (right). The ABC groove is angled in the upward direction and a clear asymmetry is visible (increased collection for the metallised side of the groove). It is also clear that the collection probability inside the groove is higher in the case of the ABC cell.

The LBIC mapping shows an asymmetry in the case of the angled grooves, as may be expected. The collection probability for long wavelength light was increased on the plated side of the groove. This suggests that the long wavelength light is neither reflected out of the cell nor absorbed at the silicon-metal interface. The

increased effective width of the cell for long wavelength light thus appears to be beneficial, since the area in which carriers will have a shorter distance to travel to the p-n junction will be increased. Despite having a physical width almost twice that of the standard buried contact, the width of the angled buried contact groove appears to be reduced in comparison to the buried contact groove.

5 CONCLUSIONS AND OUTLOOK

In summary, we have introduced an easily realisable, innovative cell design: the angled buried contact or ABC cell, which results in negligible front surface shading losses. The technical feasibility of this design has been demonstrated and the first results are promising. An increase in J_{sc} was observed, but local shunting resulted in a decrease in V_{oc} and fill factor compared to reference buried contact cells. Future work will focus on an optimisation of the groove geometry and on a more detailed study of possible light trapping benefits.

ACKNOWLEDGEMENTS

This work was done at UKON as part of the TOPSICLE project funded by the European Commission's FP5 Energy R&D programme (contract no. ENK6-CT2002-00666). Thanks to Nidia Gawehns for diffusions, Eckard Weffringhaus for SEM pictures, Axel Herguth for LBIC measurements and Helge Haverkamp for nitride depositions.

REFERENECES

- [1] S. R. Wenham, M. A. Green. (1984) Australian Patent No. 570309.
- [2] N. Mason, A. Artigao, P. Banda, R. Bueno, J.M. Fernandez, C. Morilla, R. Russell. (2004) 19th EU-PVSEC Paris, 2653-2655.
- [3] W. Jooss, M. McCann, P. Fath, S. Roberts, T.M. Bruton. (2002) 3rd World Conference on Photovoltaic Energy Conversion, Osaka, 959-962.
- [4] M. McCann, I. Melnyk, E. Weffringhaus, A. Hauser, P. Fath, S. Roberts, T. Bruton, D. Jordan. (2004) 19th EU-PVSEC Paris, 612-615.
- [5] W. Jooss, P. Fath, E. Bucher, S. Roberts, T.M. Bruton. (2001) 17th EU-PVSEC, Munich, 1727-1730.
- [6] S. Eager, N. Mason, T. Bruton, J. Sherborne, R. Russell. (2002) 29th IEEE PVSC, New Orleans, 62-65.
- [7] M.A. Green, S.R. Wenham, J. Yhao, S. Bowden, A.M. Milne, M. Taouk, F. Zhang. (1991) IEEE, 46-53.
- [8] F. Huster, S. Seren, G. Schubert, M. Kaes, G. Hahn, O. Breitenstein (2004) 19th EU-PVSEC Paris, 832-835.
- [9] M. Kaes, S. Seren, T. Pernau, G. Hahn. (2004) *Progress in Photovoltaics: Research and Applications*; **12**: 355-363.
- [10] J. Isenberg, W. Warta. (2004) *Journal of Applied Physics*; **95**: 5200-5209.